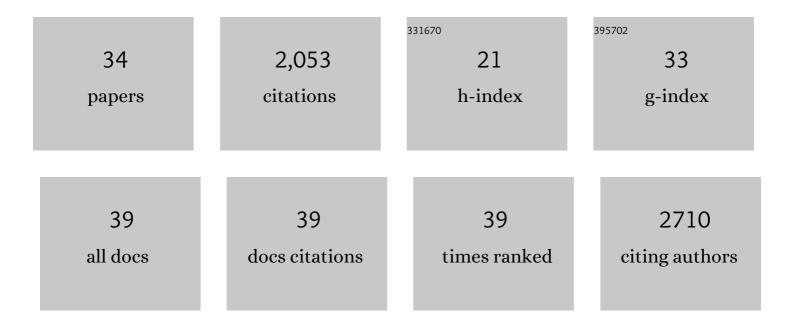
Nathan R Zaccai

List of Publications by Year in descending order

Source: https://exaly.com/author-pdf/3102234/publications.pdf Version: 2024-02-01



#	Article	IF	CITATIONS
1	Strikingly Different Roles of SARS-CoV-2 Fusion Peptides Uncovered by Neutron Scattering. Journal of the American Chemical Society, 2022, 144, 2968-2979.	13.7	30
2	FCHO controls AP2's initiating role in endocytosis through a PtdIns(4,5)P ₂ -dependent switch. Science Advances, 2022, 8, eabn2018.	10.3	14
3	Structures of a deAMPylation complex rationalise the switch between antagonistic catalytic activities of FICD. Nature Communications, 2021, 12, 5004.	12.8	13
4	Mechanism and evolution of the Zn-fingernail required for interaction of VARP with VPS29. Nature Communications, 2020, 11, 5031.	12.8	21
5	Navigating the Structural Landscape of De Novo α-Helical Bundles. Journal of the American Chemical Society, 2019, 141, 8787-8797.	13.7	42
6	Downsizing Proto-oncogene cFos to Short Helix-Constrained Peptides That Bind Jun. ACS Chemical Biology, 2017, 12, 2051-2061.	3.4	43
7	Contribution of the clathrin adaptor AP-1 subunit µ1 to acidic cluster protein sorting. Journal of Cell Biology, 2017, 216, 2927-2943.	5.2	35
8	A central cavity within the holo-translocon suggests a mechanism for membrane protein insertion. Scientific Reports, 2016, 6, 38399.	3.3	54
9	Structural Basis of the Mispairing of an Artificially Expanded Genetic Information System. CheM, 2016, 1, 946-958.	11.7	17
10	Deuterium Labeling Together with Contrast Variation Small-Angle Neutron Scattering Suggests How Skp Captures and Releases Unfolded Outer Membrane Proteins. Methods in Enzymology, 2016, 566, 159-210.	1.0	46
11	Modular Design of Self-Assembling Peptide-Based Nanotubes. Journal of the American Chemical Society, 2015, 137, 10554-10562.	13.7	137
12	Skp Trimer Formation Is Insensitive to Salts in the Physiological Range. Biochemistry, 2015, 54, 7059-7062.	2.5	20
13	Outer membrane β-barrel protein folding is physically controlled by periplasmic lipid head groups and BamA. Proceedings of the National Academy of Sciences of the United States of America, 2014, 111, 5878-5883.	7.1	164
14	Membrane protein thermodynamic stability may serve as the energy sink for sorting in the periplasm. Proceedings of the National Academy of Sciences of the United States of America, 2013, 110, 4285-4290.	7.1	104
15	A Basis Set of <i>de Novo</i> Coiled-Coil Peptide Oligomers for Rational Protein Design and Synthetic Biology. ACS Synthetic Biology, 2012, 1, 240-250.	3.8	226
16	Cryo-transmission electron microscopy structure of a gigadalton peptide fiber of de novo design. Proceedings of the National Academy of Sciences of the United States of America, 2012, 109, 13266-13271.	7.1	70
17	FKBP12 Activates the Cardiac Ryanodine Receptor Ca2+-Release Channel and Is Antagonised by FKBP12.6. PLoS ONE, 2012, 7, e31956.	2.5	56
18	A de novo peptide hexamer with a mutable channel. Nature Chemical Biology, 2011, 7, 935-941.	8.0	172

#	Article	IF	CITATIONS
19	Correlation of in situ mechanosensitive responses of the <i>Moraxella catarrhalis</i> adhesin UspA1 with fibronectin and receptor CEACAM1 binding. Proceedings of the National Academy of Sciences of the United States of America, 2011, 108, 15174-15178.	7.1	28
20	Crystal structure of a 3â€oxoacylâ€(acylcarrier protein) reductase (BA3989) from <i>Bacillus anthracis</i> at 2.4â€Ã resolution. Proteins: Structure, Function and Bioinformatics, 2008, 70, 562-567.	2.6	22
21	Single-Channel Characterization of the Rabbit Recombinant RyR2 Reveals a Novel Inactivation Property of Physiological Concentrations of ATP. Journal of Membrane Biology, 2008, 222, 65-77.	2.1	11
22	Intrinsic fluorescence as an analytical probe of virus-like particle assembly and maturation. Biochemical and Biophysical Research Communications, 2008, 375, 351-355.	2.1	11
23	Crystallographic and in Silico Analysis of the Sialoside-binding Characteristics of the Siglec Sialoadhesin. Journal of Molecular Biology, 2007, 365, 1469-1479.	4.2	30
24	Refolding of a membrane protein in a microfluidics reactor. European Biophysics Journal, 2007, 36, 581-588.	2.2	7
25	Application of high-throughput technologies to a structural proteomics-type analysis ofBacillus anthracis. Acta Crystallographica Section D: Biological Crystallography, 2006, 62, 1267-1275.	2.5	24
26	Assembly of Human Papillomavirus Type-16 Virus-Like Particles: Multifactorial Study of Assembly and Competing Aggregation. Biotechnology Progress, 2006, 22, 554-560.	2.6	32
27	The Crystal Structure of Human CD1b with a Bound Bacterial Glycolipid. Journal of Immunology, 2004, 172, 2382-2388.	0.8	137
28	Structure-Guided Design of Sialic Acid-Based Siglec Inhibitors and Crystallographic Analysis in Complex with Sialoadhesin. Structure, 2003, 11, 557-567.	3.3	97
29	Generation of CD1 tetramers as a tool to monitor glycolipid–specific T cells. Philosophical Transactions of the Royal Society B: Biological Sciences, 2003, 358, 875-877.	4.0	12
30	CD4 T Cells Selected by Antigen Under Th2 Polarizing Conditions Favor an Elongated TCRα Chain Complementarity-Determining Region 3. Journal of Immunology, 2002, 168, 1018-1027.	0.8	17
31	Structure of human CD1b with bound ligands at 2.3 Ã, a maze for alkyl chains. Nature Immunology, 2002, 3, 721-726.	14.5	234
32	Killer Cell Immunoglobulin Receptors and T Cell Receptors Bind Peptide-Major Histocompatibility Complex Class I with Distinct Thermodynamic and Kinetic Properties. Journal of Biological Chemistry, 1999, 274, 28329-28334.	3.4	110
33	HLA-B27 and disease pathogenesis: new structural and functional insights. Expert Reviews in Molecular Medicine, 1999, 1, 1-10.	3.9	10
34	Strikingly different roles of SARS-CoV-2 fusion peptides uncovered by SNR, SANS, QENS, and NSE experiments. Neutron News, 0, , 1-2.	0.2	0